

## **Influence of orographically enhanced SW Monsoon flux on coastal processes along the SE Arabian Sea**

Onkar S. Chauhan<sup>1\*</sup>, B.R. Raghavan<sup>2</sup>, Khushvir Singh<sup>3</sup>, A.S. Rajawat<sup>4</sup>, Ajai<sup>4</sup>, U. Syed Abdul Kader<sup>1</sup>, and Shailesh Nayak<sup>5</sup>

1 National Institute of Oceanography, CSIR, Dona Paula, Goa 403 004 India

2. Department of Marine Geology, Mangalore University, Mangalore, India 574199

3. India Meteorological Department, Panaji, Goa 403001 India

4. Space Application Center, P.O. SAC, Ahmedabad, 380 015 India

5. Ministry of Earth Science, CGO Complex, Lodhi Road, New Delhi, 110003 India

[1] The Arabian Sea has an excess evaporation over precipitation regime. The southeast Arabian Sea is, however, anomalous because it has ~2800-4800 mm rainfall during the southwest monsoon (SWM). Despite a high rainfall, the fluvial influence on supply of total suspended matter (TSM) and marine productivity is deemed insignificant and remains unevaluated. We evaluated the poorly resolved influence of fluvial influx on shelf processes. We documented low salinity, stratification, high productivity and turbidity over the entire inner shelf (chlorophyll-a ~2.4 mg m<sup>-3</sup>; PO<sub>4</sub><sup>3-</sup> > 2.5 μM; NO<sub>3</sub><sup>-</sup> 6.8-2.1 μM; TSM 88-182 mg l<sup>-1</sup>; salinity near shore region 26; offshore region 33.8-34.6 p.s.u.). The deeper regions (> 40 m), however, had greatly reduced TSM and nutrient levels (NO<sub>3</sub><sup>-</sup> & PO<sub>4</sub><sup>3-</sup> < 1.0 μM), TSM (< 24 mg l<sup>-1</sup>), and patches of high chlorophyll-a. Upon cessation of the SWM, nutrient levels and TSM reduced considerable. We identify two processes that contribute to the marine productivity and turbidity during the SWM. Over the deeper regions, there is a poor influence of fluvial supply and upwelling regulates productivity. Over the shallow inner shelf, the sequestering of fluvial influx due to the prevalence of strong winds, upwelling and equatorward flow is dominant. The later processes induced high marine productivity and eutrophication in the near shore region, and may have implications for siltation of channels. Reduced turbidity, nutrient and chlorophyll-a levels and higher salinity of the coastal waters during rest of the year imply a substantial role of fluvial fluxes on coastal processes.

Key words: Southwest monsoon precipitation, fluvial processes, marine productivity, anoxia, carbon sequestering, SE Arabian Sea.

\*Corresponding author.

Email: onkar@nio.org; Tel: +918322450338; Fax: +918322450609

## 1. Introduction

[2] Although influenced by the southwest monsoon (SWM), most of the Arabian Sea is deemed to have a dominant evaporation over precipitation ( $E \gg P$ ) regime [Chauhan *et al.*, 2010 and references therein]. By virtue of the existence of a regional topographic high, the “Western Ghats” (which facilitates the excessive condensation of moisture from the SWM winds upon their reaching land), the entire southwestern continental margin of India (the SE Arabian Sea) has excess precipitation south of  $15^\circ\text{N}$  along the west coast of India ( $\geq 2700 - 4800$  mm) during the SWM. The hinterland of the northeast Bay of Bengal is another such region in the northern Indian Ocean [Sarker 1966; Xie *et al.*, 2006]. Although there is intense rainfall in both these regions [Xie and Arkin, 1997], in contrast to the Bay of Bengal, the SW continental margin of India has been considered insignificant in terms of fluvial discharge [Vörösmarty *et al.*, 1996; Yu and McCreary, 2004], perhaps due to the existence of very small and seasonal rivers. It has been speculated that the fluvial contribution to the SE Arabian Sea is insignificant in the sustaining of high coastal productivity or excessive subsurface carbon flux [Vörösmarty *et al.*, 1996; Naqvi *et al.*, 2009 and references therein]. During the SWM, there is an incessant rainfall over the western flank (sloping towards the Arabian Sea) of the Western Ghats [Chauhan *et al.*, 2010]. Because of high elevation ( $\sim 2000$  m) and the Precambrian mountainous terrain, most of this rainwater finds its way into the Arabian Sea through a network of high gradient rivers [Chauhan and Gujar, 1996]. There is a paucity of data on the discharge magnitude and nutrient input of SWM-fed rivers into the sea from this region. Along the southern stretches of the SW coast of India, Chandramohan and Balachand [2007] have estimated fluvial discharge into the SE Arabian Sea. This study found  $\sim 324$  km<sup>3</sup> discharge during the SWM (June through September), and  $\sim 112$  km<sup>3</sup> during the non-monsoon season (October through May) from 16 local rivers. Being located in the similar meteorological and physiographic terrain, the entire region is expected to have equitable high seasonal fluvial influx. Understanding the fate of such a large fluvial fluxes is important because (i) being a regional phenomenon these persist over the entire SE Arabian Sea; (ii) they are regulated only by the magnitude of the SWM; (iii) they carry anthropogenic nutrients, insecticides, pesticides and sewage into the sea from the littoral states; and (iv) they influence optical properties of sea waters, marine productivity and anoxia or hypoxia, which are crucial factors affecting the coastal food web and carbon sink mechanisms.

[3] Under a national initiative of the Space Application Center of the Indian Space Research Organization (ISRO), the present work was a modest beginning to evaluate the influence of fluvial fluxes on coastal processes. Because of operational limitations in carrying out synchronous

measurements over the entire SE Arabian Sea, a representative region (395 km long and 100 km wide; geographic location 13-15.3°N; 73.3-75°E) was selected for close grid studies. The study area is located in a region with a vigorous SWM regime in which precipitation is enhanced by orography (Table 1), and this precipitation is carried nearly instantaneously into the sea by several small high-gradient rivers (Figure 1). Month-scale, validated, imagery-derived chlorophyll-a and TSM were obtained. Dedicated in situ measurements during the SWM (August) and the post monsoon season (January-February) were also made. Synchronous salinity, nutrients, temperature and current measurements were also performed. The surface and the subsurface variations in chlorophyll-a, nutrients ( $\text{NO}_3^-$  and  $\text{PO}_4^{3-}$ ), salinity and dissolved  $\text{O}_2$  (DO) were used to assess the poorly resolved influence of SWM-related fluvial fluxes on coastal productivity, eutrophication and anoxia.

## 2. Study Area

[4] As indicated earlier, the southwest continental margin of India has incessant rains. Originating from the Western Ghats, numerous small rivers debouch into the sea (Figure 1). The average salinity of the Arabian Sea is generally high owing to the prevalence of excessive evaporation regime ( $E \gg P$ ; [Chauhan *et al.*, 2010]). The fluvial discharge during the SWM, however, reduces the regional sea surface salinity to 33.8-34.6 practical salinity units (p.s.u.) in the deeper regions, [Levitus *et al.*, 1994; Figure 1 (inset)], and  $\sim 26$  p.s.u. in the near-shore regions along the SE Arabian Sea. The hydrography of the region is seasonal. During the SWM (June through September), the Indian Monsoon Current (also known as the West India Coastal Current) carries the high-salinity Arabian Sea water into the Bay of Bengal through equatorward flow [Kumar *et al.*, 2004]. Strong winds induce upwelling over deeper regions of the continental margin [Naqvi *et al.*, 2009]. Upon cessation of the SWM, there is no upwelling, and the flow is poleward. Furthermore, the area is mesotidal, and a high wave regime prevails during the SWM (waves height of  $> 2.5$  m for about 40 % of the time, wave period ( $T$ ) =  $> 8$  sec for about 60 %; [Varkey *et al.*, 1982]) due to the intense wind regime (0.7 dyne/sec; [Habebrehman *et al.*, 2008]). Waves and winds are moderate (wave height of  $< 2.0$  m about 85 % of the time  $T = < 8$  sec for 80%; [Varkey *et al.*, 1982]) during rest of the year.

## 3. Methodology

[5] We obtained and analyzed daily precipitation data from two available meteorological stations, (i) Karwar (District: Kanara North 14° N 74° E) and (ii) Mangalore (District: Kanara South: 12° N: 74° E), between 2001 and 2005. These stations are, however, located at the coast, and not in the hills. Because the rainfall in this region is regulated by the orography, the rainfall magnitude of these stations may be

lesser compared to the actual rainfall in the inland hilly region. Data on the average monthly rainfall, the total number of rainy days and the daily highest precipitation were obtained (Table 1). These data suggest high seasonal rainfall. There are several small rivers debouching into the study area (Figure 1). Because the rivers of the Western Ghats are mostly rain-fed [*Chandramohan and Balchand, 2007*], and the habitation is mostly confined to the narrow coastal strips, the discharge magnitude of the rivers is expected also to be regulated mainly by precipitation.

[6] TSM estimation was performed according to the protocol of JGOFS (matter retained on <0.45- $\mu$ m Opti pure fiber filter paper; [*UNESCO 1994*]). To strengthen the field observations we used the Indian Remote Sensing Ocean color monitor (IRS-P4 OCM) data for path-09 row-13 (spectral channel central wavelength [bandwidth]: 412[20], 443[20], 490[20], 510[20], 555[20], 670[20], 780[40], 860[40] nm; spatial resolution: 0.36 km; payload altitude: 760 km; recurrent period: 2-days; satellite overpass: 1200 $\pm$ 0020 hrs LST). After making the necessary atmospheric and geometric corrections [*Prasad et al., 2002*], the modified algorithm for IRS P-4 OCM products [*SAC Report, 2004*] and SeaWiFS Data Analyses Software [*SAC Report, 2004*] were used to process the images from the following relations:

$$\text{Log (S)} = 1.83 + 1.26 \text{Log} (\chi S) \quad \forall 0.0 \leq S \leq 40.0$$

where S is suspended sediment concentration ( $\text{mg l}^{-1}$ ) and  $\chi S$  is a variable defined as:

$$\chi S = [\text{Rrs} (555) + \text{Rrs} (670)] \times [\text{Rrs} (555) / \text{Rrs} (490)]^{0.5}$$

where Rrs ( $\lambda$ ) is the remote sensing reflectance at the respective wavelength ( $\lambda$ ). The reported retrieval accuracy of TSM from OCM data is  $\pm 15\%$  [*SAC Report, 2004*]. Considering the strong seasonality in the river discharge, we have obtained month specific variability in the TSM during 2003-2004. Because of intense and persistent cloud cover we could obtain only a limited number of cloud-free scenes during the SWM seasons of 2003-2004, and week-scale resolution could not be maintained. Because of the high number of rainy days ( $\geq 20$ ) and near constant discharge magnitude of the rivers during the SWM in this region [*Chandramohan and Balchand, 2007*], we expect very small temporal variability in the magnitude of nutrients and TSM flux during the SWM season.

[7] At 118 stations, multiplatform, mid-tide synchronous water sample collection and in situ measurements were carried out during August of 2004 for estimation of chlorophyll-a, TSM and nutrient variability for the SWM specific distributions (Figure 1). Persistent inclement weather limited the sampling density in very shallow and deeper offshore waters ( $> 30$  m water depth), and we could obtain only 12 vertical profiles (Figure 1). Due to logistic limitation and limited availability of platforms, these stations were revisited again in January – February of 2011 for the non-SWM specific

measurements. We have obtained month-scale TSM and chlorophyll-a variations derived through imagery to estimate if there was any significant inter-seasonal variability in these parameters. We have found high seasonality and two prominent trends in these data. During the SWM, in the shallow coastal waters there was high TSM and chlorophyll-a, which dwindled and remained similar upon cessation of the SWM. The available monthly data during the SWM had almost similar magnitude of the river discharge [*Chandramohan and Balchand, 2007*]. Although many fold lower for the non-SWM months, the fluvial discharge magnitude showed little temporal variability [*Chandramohan and Balchand, 2007*]. We therefore speculate that there is insignificant month-scale variability in fluvial discharge during the SWM and the non-monsoon months, and our measurements of August (2004) and January – February (2011) represent the SWM and the post SWM environments.

[8] Salinity and temperature data have been collected using a Hydrosonde DS-5 system of Hach Inc. at 65 stations. The subsurface measurements have been carried out along transects I and III (Figure 1). The measurements were recalibrated against conductivity standards (0.1, 0.5, 12.856 and 47.6 mS/cm of Hach Inc). Precision of the analysis against these standards was found to be better than 5%. Currents were measured synchronously at each station using CONtrol current meters (accuracy  $\pm 5\%$ ) at the surface (2 m). Advection vectors may be a good indicator of the dispersal magnitude of TSM. Real-time vectors (at 65 stations; Figure 1) were estimated from the following relation:

$$\mathbf{AD} = \mathbf{S F}$$

Where AD = advection vector ( $\text{mg m}^{-2} \text{ sec}^{-1} \text{ dir}$ );

S=TSM ( $\text{g l}^{-1}$ ); F = flow ( $\text{m sec}^{-1}$ ); direction of surface flow (0-359<sup>0</sup>)

[9] Samples from 65 stations during the SWM and during the post SWM season (Figure 1) were analyzed for  $\text{NO}_3^-$  and  $\text{PO}_4^{3-}$  using the methods of *Grasshoff et al.* [1983]. Dissolved oxygen (DO) levels were estimated using a titration method [*Strickland and Parsons, 1979*]. One liter of seawater was filtered using a 47-mm GF/F Millipore filter paper (0.7  $\mu\text{m}$  pore size), and chlorophyll-a concentrations were determined as per the JGOFS protocol [*UNESCO, 1994*]. The precision of all these analyses was about  $\pm 5\text{-}7\%$ . A regional synoptic view of the monthly chlorophyll-a abundance was obtained also from available cloud-free satellite images taken during the years 2003-2004 using the following relation [*Chauhan et al., 2002*]:

$$C = 10^{(0.319 - 2.336R + 0.879R^2 - 0.135R^3) - 0.071} \text{ for } 0.01 \leq C \leq 50 \text{ (mg m}^{-3}\text{)}$$

where, C= chlorophyll-a concentration ( $\text{mg m}^{-3}$ )

$R = \log_{10} \{Rrs(490)/Rrs(555)\}$ , and

*Rrs*= remote sensing reflectance

#### 4. Results

[10] The monthly precipitation variability and the number of rainy days per month are presented in Table 1. Overall, the area received ~ 2700 mm rainfall and had a high number ( $\geq 20$ ) of rainy days during the SWM. About 80% of the yearly rainfall occurs during the SWM. There were instances of isolated post-monsoon rains during October and January of 2001. Such rainfall was, however, insignificant in terms of influencing the discharge of the rivers (Table 1).

[11] The spatial distribution of TSM during the SWM and the post SWM periods is presented in Figure 2. Imagery-derived, month-scale variability in TSM (during 2004) is also presented in Figure 3. The shallow inner shelf waters were highly and uniformly turbid for about 25 km ( $\text{TSM} > 88 \text{ mg l}^{-1}$ ) during the SWM. The mid-outer shelf had reduced TSM (12- 24  $\text{mg l}^{-1}$ ). The boundary between these two water bodies was distinct and present at 35-40-m isobaths during the SWM and shifted landwards upon cessation of the SWM. Round the year, in the waters deeper than 40 m, we found no significant decrease in the TSM level. The imagery-derived TSM patterns mimicked the measured trend (Figures 2-3) and supported the existence of a distinct regional boundary at ~ 35 m during the SWM. We have observed a landward migration of TSM enriched zone upon cessation of the SWM. The imagery-derived TSM values for the coastal waters were, however, underestimated in the shallow regions. The available algorithms are known to underestimate TSM in Case II coastal waters [*Tassan, 1994; SAC report, 2004*]. Therefore, the synoptic pattern in the shallow case II waters is only a qualitative confirmation of the pattern derived from the in situ measurements.

[12] The distributions of chlorophyll-a, nutrients and DO are presented in Figures 4-8. The shallow coastal waters and the deeper offshore waters were found to be productive during the SWM (chlorophyll-a  $> 2 \text{ mg m}^{-3}$  over the inner shelf;  $\geq 1.2 \text{ mg m}^{-3}$  over the deeper waters; Figure 4). Upon cessation of the SWM, however, the chlorophyll-a abundance reduced in shallow waters ( $< 0.6 \text{ mg m}^{-3}$ ; Figure 4). The nitrate distribution had a distinct spatial variability during the SWM. Low nitrate concentrations were found in the mid-outer shelf waters, and the inner shelf had elevated nitrate levels (6.8-2.1  $\mu\text{M}$ ; Figure 5). Upon cessation of the SWM, we have found much reduced nutrient levels in the shallow coastal waters (Figure 5). Vertical profiles of nitrate were also diverse (Figures 7-8). In contrast to the downward decreasing trend in the shallow coastal waters, the mid-outer shelf waters were enriched in  $\text{NO}_3^-$  at deeper subsurfaces during the SWM (~24.6–15  $\mu\text{M}$ ; Figure 7). During the post SWM, however, this trend was not seen (Figure 8). DO varied between 0 and 198  $\mu\text{M}$ , and surface

waters, by and large, were enriched in DO. The deeper subsurfaces over the mid-outer shelf were very deficient in DO, and hypoxia prevailed in these regions during the SWM (Figures 7). The subsurface DO deficiency was also observed in the shallow coastal region, though the magnitude of this deficiency (20  $\mu\text{M}$ ) was less than that of the deeper waters (Figure 7). During the post SWM, the coastal as well as the deeper waters were having higher surface and subsurface DO levels (Figures 6, 8).

[13] Currents were moderate to strong (22-72  $\text{cm sec}^{-1}$ ) in the inland and in the offshore waters (Figure 9). The current direction was predominantly alongshore (equatorward) and was consistent with the reported flow during the SWM [Kumar *et al.*, 2004 and references therein]. Upon cessation of the SWM, current direction was polewards. Sustained by the SWM and the post SWM currents, advection of TSM was alongshore for the entire region (Figure 9). The magnitude of advection, however, was different at the inner and the outer shelves. Compared to the deeper regions, the inner shelf had a many-fold higher magnitude of advection (26-110  $\text{mg m}^{-2} \text{sec}^{-1}$  for < 40 m water depth; 4-9  $\text{mg m}^{-2} \text{sec}^{-1}$  for the deeper region) during the SWM. Upon cessation of the SWM, except at the localized regions off the mouth of the rivers, we found much reduced advection rates over the entire shelf (Figure 9).

## 5. Discussion

[14] As indicated earlier, along the SE Arabian Sea, no real-time measurements of the magnitude and dispersal pathways of fluvial flux exist over the continental margin. It has perhaps been presumed that fluvial discharge is rather small and that it carries insignificant quantities of terrigenous matter and nutrients into the sea. We rely upon the reported fluvial discharge (16 rivers) from the adjacent southern region of the SE Arabian Sea. The individual discharge of these rivers varied between 6895-701  $\text{m}^3 \text{sec}^{-1}$  which contributed to about  $\sim 324 \text{ km}^3$  fluvial discharge during the SWM and  $\sim 112 \text{ km}^3$  discharge during the non-monsoon months [Chandramohan and Balchand, 2007]. An intense SWM precipitation regime (rainy days  $\geq 20 \text{ month}^{-1}$ ; Table 1) appeared to sustain a persistent fluvial flow, which reduced the regional salinity (Figure 10). Raghavan and Chauhan [2011] have estimated nutrients ( $\text{PO}_4^{3-}$  and  $\text{NO}_3^-$ ) in the River Kali located in the northern region of the study area (Figure 1). This study suggests 3.6-6.8  $\mu\text{M}$  nitrate during the SWM, which reduces to 0.4-2.6  $\mu\text{M}$  upon cessation of the SWM. Phosphate content in the river was 0.8-2.8  $\mu\text{M}$  and 0.2-1.6  $\mu\text{M}$  during the SWM and the non-SWM months respectively. TSM had a large seasonal variability, and it was 102-182  $\text{mg l}^{-1}$  and 12-28  $\text{mg l}^{-1}$  during the SWM and the non-SWM in the fluvial load [Raghavan and Chauhan, 2011]. These data suggest a high TSM and nutrient load in the river. The prevalent tropical climate and high population density appeared to bolster high TSM yield. Recent deforestation associated with the construction of a

mega atomic power plant, a naval base and the unplanned expansion of several coastal townships due to demographic pressure appears to have contributed to the turbidity of the rivers. Even though some entrainment is common in the estuarine region, we assumed an instantaneous supply of the fluvial flux into the sea because of the hilly terrain, the high gradient and the short length of these rivers. Reduced TSM in the rivers during the non-SWM season implied that the yield and supply of TSM into the sea had a link with SWM precipitation.

[15] Being a major constituent of the river load, we used TSM as a natural tracer to determine the dispersal and sink pathways of fluvial flux into the SE Arabian Sea. We observed high turbidity over the entire inner shelf (TSM 88-182  $\text{mg l}^{-1}$ ) during the SWM. In contrast, the deeper regions of the shelf had low TSM levels (12-24  $\text{mg l}^{-1}$ ; Figures 2-3). The spatial extent of turbid water shrunk closer to the shore upon the termination of the SWM. Irrespective of seasonal variability in the fluvial flux, we have found no change in the amount of TSM over the deeper region of the shelf year round. The amount of TSM in the seawaters of the Arabian Sea has been linked with the SWM [Nair *et al.*, 1989; Haake *et al.*, 1993; 1996; Rixen *et al.*, 2009 and references therein]. However, two contrasting trends in our study area prevailed during the SWM when the fluvial flux was at a maximum. Because the amount of TSM did not change upon cessation of the SWM in the deeper regions of the shelf (Figures 2-3), we infer that the flux magnitude alone does not play a major role in the spatial variations in the TSM over the continental margin of the SE Arabian Sea. We speculate a role for the morphodynamic regime.

[16] We evaluated the current and wind regimes (averaged bimonthly for, June through September for SWM and November through February of 2004 for the non-monsoon season) at a  $0.25^\circ$  grid (data source: <ftp://ftp.ifremer.fr/pub/ifremer/cersat/products/gridded/mwf-quikscat/data/monthly/>) to determine their influence on the dispersal and sequestering pathways of TSM. Moderate–strong alongshore currents accompanied with strong winds prevailed during the SWM (Figures 9, 11). Upon cessation of the SWM, the winds were mild, but the currents were moderate – strong. Wind plays a vital role in dispersal and sequestering of the fluvial flows over the continental margin [Liu and Weisberg, 2005, 2007; Liu *et al.*, 2009]. Study area has a vigorous wind from offshore during the SWM (near W-NW; Figure 11), which appears to aid in sequestering of TSM in the coastal regions by piling up and downwelling waters in the shallow region of the shelf. Such a wind regime is found favorable also for alongshore (equatorwards) displacement of seawater [Muraleedharn and Kumar, 1996]. High density of small, high gradient rivers, fed by orographically enhanced precipitation discharge a large amount of freshwater (fluvial discharge  $\sim 324 \text{ km}^3$  during the SWM [Chandramohan and Balchand, 2007]). Because the



prevailing wind during the SWM piles the water up at the coast as well as equatorwards flow, it aids in along-shelf expansion by merging the flow of several of the small rivers. This sequesters fluvial discharge along the coast, reduces salinity of the shallow coastal waters and curtails offshorewards advection of fluvial plumes during the SWM. We have evaluated temperature and salinity (T-S) profiles during the SWM and the post-monsoon seasons to assess this thesis further. We found reduced salinity (26-34.6 p.s.u.) in surface and 0-20 m subsurfaces in shallow coastal waters (Figure 10), a result similar to those of other studies [*Habeebrehman et al.*, 2008; *Naqvi et al.*, 2009]. The reduced surface and subsurface salinity (~ 0-20 m sublevels) during the SWM implies that the fluvial flux sequesters and percolates into the deeper subsurfaces due to prevalent downwelling favorable wind regime. Upon cessation of the SWM, the salinity is enhanced and there is no subsurface salinity reduction in the shallow coastal waters (Figure 10), which may be attributed to a poor fluvial discharge and the feeble alongshore wind unfavorable either to pile up water up shore or for a strong alongshore flow required for sustaining upwelling. Endorsement to this inference is derived from the temperature profile, which shows down-sloping of the isotherm (downwelling) in the shallow coastal waters (0-20 m depth; Figure 10). The temperature and salinity profiles are, however, different at the deeper region (> 50 m; Figure 10), and we have found up-sloping of isotherms. Similar trend was seen in the nitrate distribution (Figure 7). These trends had lead us to infer an occurrence of upwelling in the region deeper than 50 m during the SWM. We obtained also a sea surface anomaly for the SWM season of 2004 (<http://atoll-motu.avisioceanobs.com/?action=listcatalog&service=AvisoDT>). The entire deeper region of the shelf had a negative anomaly (Figure 12), which we attribute to the prevalence of intense upwelling. An intense upwelling in the deeper waters of the SE Arabian Sea has been reported in other studies [*Naqvi et al.*, 2009 and references therein]. This upwelling pumps deeper, cold waters into the upper subsurfaces, which is not conducive to across-shelf advection of TSM. During the SWM, the sequestering of the fluvial fluxes over the inner shelf stems therefore from the prevalent alongshore currents, the strong near across-shelf winds and the upwelling regime. This hypothesis is supported further by the higher advection rates of TSM in the shallow waters (26-110 mg m<sup>-2</sup> sec<sup>-1</sup>) compared to the deeper region (4-9 mg m<sup>-2</sup> sec<sup>-1</sup>) during the SWM.

[17] We evaluated the influence of SWM fluvial flux on marine productivity. Nutrient availability is a crucial factor for marine productivity. Because of the paucity of data from the shallow coastal region (< 20 m), the supply of nutrients and hypoxia in the SE Arabian Sea has been linked mostly to hydrography-induced upwelling from 100-200 m deep subsurfaces during the SWM [*Devol et al.*, 2006;

*Naqvi et al.*, 2006, 2009 and references therein]. These upwelled waters were characterized by a specific nutrient profile, i.e., a progressive upward depletion in nutrient availability [*Devol et al.*, 2006; *Naqvi et al.*, 2006; 2009], and a well-defined T-S profile. Over the inner shelf (in the shallow coastal waters), we found nutrient enrichment ( $\text{NO}_3^-$  and  $\text{PO}_4^{3-}$ ) in the upper surfaces, though the deeper subsurfaces in this region had reduced salinity, and were depleted in  $\text{NO}_3^-$  (Figures 7, 10). Such a vertical nutrient and T-S distributions were not consistent with the trend observed for the deeper region, in which  $\text{NO}_3^-$  showed progressive subsurface enrichment with a maximum at >50 m (Figures 7, 10) along with cooler temperature (isotherm upturning) and prevalence of high salinity in these subsurfaces. Such a distribution is not found during the post SWM season (Figure 10). Similar to other studies [*Devol et al.*, 2006; *Naqvi et al.*, 2000, 2006, 2009], the trend observed in our study during the SWM (over the deeper waters) may be attributed to the upwelling, which is the major source of nitrate in this region. Because a high temperature, low nitrate, and salinity in the deeper subsurfaces in the shallow waters conflict with the pattern of these indices in the deeper offshore waters (Figures 7, 10), we attribute these trends to the sequestering of the local fluvial flux due to the prevalent wind regime.

[18] At about 25 km inland, the nitrate level varied between 2.1 and 6.8  $\mu\text{M}$  in the local river, which reduced to 1.9-3.2  $\mu\text{M}$  during the post SWM season [*Raghavan and Chauhan*, 2011]. The SWM is a prominent harvesting season, and farmers in the coastal region (with extensive cultivation) use a large amount of chemical fertilizer in the region downstream to the sampling locations of *Raghavan and Chauhan* [2011]. The measurement of nitrate in a single river appears inadequate to quantify the nitrate flux into the sea from the fluvial process. The available data are therefore useful only to provide a qualitative indication of the magnitude of the fluvial fluxes from the SWM regime. The paucity of data has hindered our efforts to quantify the nitrate flux or the coastal productivity induced by the SWM fluvial flux using the Redfield ratio. As an alternative, comparison of the nutrient variability during the SWM and in the post-monsoon season in the coastal waters has been used for approximation of the nutrient supply during the SWM. Upon cessation of the SWM, substantial decreases in  $\text{NO}_3^-$  and  $\text{PO}_4^{3-}$  concentrations have been observed over the inner shelf (SWM nitrate 2.5-6.8  $\mu\text{M}$ ; post monsoon 0.7-2.4  $\mu\text{M}$ ; SWM phosphate >2.5; post monsoon  $\sim 0.4 - 1.1 \mu\text{M}$ ; Figures 7-8). *Shirodkar et al.* [2009] had also found equitable nutrients during the post monsoon season. A considerable reduction in the nutrient concentrations upon cessation of the SWM in the shallow coastal waters, therefore, appears to be linked with the magnitude of the fluvial discharge.

[19] Sustained mostly by nutrient availability, chlorophyll-a is considered to be an index of primary productivity [Banse, 1987]. We observed high chlorophyll-a levels ( $\sim 2.4 \text{ mg m}^{-3}$ ) all along the shallow inner shelf not characterized by upwelling, during the SWM (with a subsurface maximum at  $\sim 12 \text{ m}$ ), which may be attributed to a favorable fluvial nutrient flux into the region (Figures 3-4). Regulated by the magnitude and the direction of the prevailing wind, the variable upward nutrient supply from deeper subsurfaces through Ekman pumping (upwelling), appears to sustained high but a patchy surface chlorophyll-a distribution (with a subsurface maximum at 12-16 m) over the mid-outer shelf (water depth  $> 50 \text{ m}$ ), the regions characterized by a low TSM in seawater. The amount of chlorophyll-a reduces considerably upon cessation of the SWM in the shallow as well the deeper regions of the shelf ( $< 0.6 \text{ mg m}^{-3}$ ; Figures 3- 4). We link the patterns of chlorophyll-a over the inner and the outer shelves during the SWM to the influence of the fluvial and the hydrographic processes, respectively.

[20] DO is a measure of anoxia and hypoxia [Naqvi *et al.*, 2010]. DO in seawater is supplied through air-sea interactions and primary productivity. Being in dynamic equilibrium with the atmosphere, upper sea surfaces are expected to be well oxygenated. Strong mixing is also known to percolate  $\text{O}_2$  into deeper subsurfaces and to ventilate deeper waters [Sardessai *et al.*, 2007]. Consumption of  $\text{O}_2$  due to subsurface flux of organic matter is considered a major cause of  $\text{O}_2$  depletion [Naqvi *et al.*, 2009 and references therein]. Additionally, land-derived natural and anthropogenic organic carbon fluxes carried in the rivers are known also to consume DO in coastal waters [Desa *et al.*, 2005]. Over the mid-outer shelf, the DO concentration in the upper surfaces during the SWM was 140-190  $\mu\text{M}$  (Figure 6), which is comparable to the values reported by Devol *et al.* [2006] and Naqvi *et al.* [2006] from the SE Arabian Sea. The shallow coastal waters, however, had reduced DO levels (84-120  $\mu\text{M}$ ), which had diminished further in the deeper subsurfaces ( $\sim 20 \mu\text{M}$ ; Figures 6-7). Over the mid-outer shelf, subsurface depletion was rather rapid and was similar to that reported in other studies [Devol *et al.*, 2006; Naqvi *et al.*, 2006]. Hypoxia occurred at the subsurfaces deeper than 50 m (Figure 7). Upon cessation of the SWM, the trend of DO distribution is markedly different. We found marginally elevated DO in the coastal waters, and no hypoxia prevailed at the deeper subsurface over the shallow as well deeper regions of the entire shelf (Figures 6, 8). We deduce, therefore, that two processes regulate the consumption of  $\text{O}_2$  over the inner and the outer shelves during the SWM. From the occurrence of lower salinity over the entire inner shelf, even in the deeper subsurfaces (Figure 10), we infer a role for fluvial supply over the inner shelf during the SWM. Strong wind during the SWM appears to have ventilated and replaced consumed  $\text{O}_2$  in deeper subsurfaces. We link the low DO levels over the inner shelf during the SWM with (i) enhanced marine

productivity supported by fluvial nutrient supplies and (ii) consumption of DO by organic matter carried in the riverine discharge. In contrast, marine productivity sustained by hydrographic upwelling [Devol *et al.*, 2006; Naqvi *et al.*, 2006, 2009], and the reduced ventilation of deeper waters appear to induce stronger hypoxia over the deeper regions of the SE Arabian Sea.

[21] In conclusion, we documented considerable discharge of nutrients and suspended matter into the SE Arabian Sea sustained by the orographically enhanced and persistent SWM precipitation. The SWM climatology with strong wind from offshore aids in the sequestering of fluvial fluxes over the inner shelf and enhances marine productivity. The sequestering of SWM fluvial discharge may have implications for eutrophication and anoxia in the fragile ecosystem of the coastal region. Coupled with the recent growth in the demand for land for neo-urbanization, agriculture, and aquaculture, further augmentation in anthropogenic loading is likely. These activities may enhance the supply of anthropogenic chemicals, nutrients, and carbon into the sea. Though it appears favorable for sustaining high marine productivity, such loading may increase surface and subsurface fluxes of organic carbon. We advocate a vigorous monitoring of the coastal habitat to preserve the existing dynamic equilibrium among biogeochemical processes to sustain the crucial marine food supply for the local population.

**Acknowledgements.** Authors acknowledge the director of the National Institute of Oceanography for providing facilities. They thank Wajih Naqvi for help in the interpretation of the nutrient and DO data. Authors express their gratitude to Professor Chunzai Wang, the Editor, and two anonymous referees for helping them improve the science in the manuscript. Authors are grateful to the Indian coast guard for their support during data collection at sea. They acknowledge the research grant from IGBP-ISRO and the Space Application Center. NIO Contribution NO XXXX.

## References

- Banse, K. (1987), Seasonality of phytoplankton chlorophyll in the central and northern Arabian Sea, *Deep-Sea Res.*, *34*, 713–723, doi:10.1016/0198-0149(87)90032-X.
- Chandramohan, T. and Balachand, A.N. (2007), Regional sediment yield pattern for the west flowing rivers of Kerala State, India, *RMZ Material and Geoenvi.*, *54*, 501-511.
- Chauhan, O. S., E. Vogelsang, N. Basavaiah, and U. S. A. Kader (2010), Reconstruction of the variability of the southwest monsoon during the past 3 ka, from the continental margin of the southeastern Arabian Sea, *J. Quaternary Sci.*, *25*(5), 798–807, doi: 10.1002/jqs.1359.

- Chauhan, O. S., and A. R. Gujar (1996), Surficial clay mineral distribution on the southwestern continental margin of India: evidence of input from the Bay of Bengal, *Cont. Shelf Res.*, *16*, 321-333, doi:10.1016/0278-4343(95)00015-S.
- Chauhan, P., M. Mohan, R. K. Sarangi, B. Kumari, S. R. Nayak, and S. G. P. Matondkar (2002), Surface chlorophyll estimation in the Arabian Sea using IRS-P4 OCM Ocean Color Monitor (OCM) satellite data, *Int J. Remote Sens.*, *23*(8), 1663–1676, doi: 10.1080/01431160110075866.
- Desa, E., M. D. Zingde, P. Vethamony, M. T. Babu, S. N. DeSousa, and X. N. Verlecar (2005), Dissolved oxygen - A target indicator in determining use of the Gulf of Kachchh waters, *Mar Pollut Bull.*, *50*(1), 73-79, doi:10.1016/j.marpolbul.2004.08.014.
- Devol, A. H., A. G. Uhlenhopp, S. W. A. Naqvi et al., J. A. Brandes, A. Jayakumar, H. Naik, S. Gaurin, L. A. Codispoti, and T. Yoshinari (2006), Denitrification rates and excess nitrogen gas concentrations in the Arabian Sea oxygen deficient zone, *Deep-Sea Res Pt I.*, *53*, 1533–1547, doi:10.1016/j.dsr.2006.07.005.
- Grasshoff, K., M. Ehrhardt, and K. Kremling (1983), *Methods of Seawater Analysis*, Verlag Chemie, New York.
- Haake, B., V. Ittekkot, T. Rixen, V. Ramaswamy, R. R. Nair, and W. B. Curry (1993), Seasonality and interannual variability of particle-fluxes to the deep Arabian Sea, *Deep-Sea Res. ptI*, *40*(7), 1323-1344, doi:10.1016/0967-0637(93)90114.
- Haake, B. T. Rixen, T. Reemtsma, V. Ramaswamy, and V. Ittekkot (1996), Processes determining seasonality and interannual variability of settling particle fluxes to the deep Arabian Sea, in *Particle flux in the ocean*, edited by V. Ittekkot, et al., SCOPE, John Wiley and Sons, Chichester, *57*, pp. 251-270.
- Habeebrehman, H., M. P. Prabhakaran, J. Jacob, P. Sabu, K. J. Jayalakshmi, C. T. Achuthankutty, and C. Revichandran (2008), Variability in biological responses influenced by upwelling events in the Eastern Arabian Sea, *J. Mar Syst.*, *74*, 545-560, doi:10.1016/j.jmarsys.2008.04.002.
- Kumar, P. S., J. Narvekar, A. Kumar, C. Shaji, P. Anand, P. Sabu, G. Rijomon, J. Josia, K. A. Jayaraj, A. Radhika, and K. K. C. Nair (2004), Intrusion of the Bay of Bengal water into the Arabian Sea during winter monsoon and associated chemical and biological response, *Geophys. Res. Lett.*, *31*, L15304, doi: 10.1029/2004GL020247.
- Levitus, S., R. Burgett, and T. P. Boyer (1994), *World Ocean Atlas: Salinity*, NOAA Atlas NESDIS, *3*, U.S. Gov. Printing Office, Wash., D.C., pp. 99.
- Liu, Y. and R. H. Weisberg (2005), Momentum balance diagnoses for the West Florida Shelf, *Cont. Shelf Res.*, *25*, 2054-2074.
- Liu, Y. and R. H. Weisberg (2007), Ocean Currents and Sea Surface Heights Estimated across the West Florida Shelf, *J. Phys. Oceanogr.*, *37*, 1697-1713.

- Liu, Y., P. MacCready, and B. M. Hickey (2009), Columbia River plume patterns in summer 2004 as revealed by a hindcast coastal ocean circulation model, *Geophys. Res. Lett.*, *36*, L02601, doi:10.1029/2008GL036447.
- Muraleedharan, P.M., and P.S. Kumar (1996), Arabian Sea upwelling – a comparison between coastal and open ocean regions, *Cur. Sci.*, *71*, 842-846.
- Nair, R. R., V. Ittekkot, S. J. Manganini, V. Ramaswamy, B. Haake, E.T. Degens, B.N. Desai, and S. Honjo (1989), Increased particle flux to the deep ocean related to monsoon, *Nature*, *338*, 749–751. doi:10.1038/338749a0.
- Naqvi, S. W. A., H. W. Bange, L. Farias, P. M. S. Monteiro, M. I. Scranton, and J. Zhang (2010), Marine hypoxia/anoxia as a source of CH<sub>4</sub> and N<sub>2</sub>O, *Biogeosciences*, *7*(7), 2159-2190, doi:10.5194/bg-7-2159-2010.
- Naqvi, S. W. A., H. Naik, A. Jayakumar, A. K. Pratihary, G. Narvenkar, S. Kurian, R. Agnihotri, M. S. Shailaja, and P. V. Narvekar (2009), Seasonal anoxia over the western Indian continental shelf, in *Indian Ocean biogeochemical processes and ecological variability*, edited by J. D. Wiggert et al., Geophysical Monograph Series, American Geophysical Union, Washington, DC, USA, 185, pp. 333-345.
- Naqvi, S. W. A., H. Naik, A. Pratihary, W. D'Souza, P. V. Narvekar, D. A. Jayakumar, A. H. Devol, T. Yoshinari, and T. Saino (2006), Coastal versus open-ocean denitrification in the Arabian Sea, *Biogeosciences*, *3*, 621–633.
- Naqvi, S. W. A., D. A. Jayakumar, P. V. Narvekar, H. Naik, V. V. S. S. Sarma, W. D' Souza, S. Joseph, and M. D. George (2000), Increased marine production of N<sub>2</sub>O due to intensifying anoxia on the Indian continental shelf, *Nature*, *408*, 346–349, doi:10.1038/35042551.
- Prasad, J. R., A. S. Rajawat, Y. Pradhan, O. S. Chauhan, and S. R. Nayak (2002), Retrieval of sea surface velocities using sequential ocean colour monitor (OCM) data. *Proc.. Indian Acad. Sci.*, *11*, 189–195.
- Raghavan, B. R., and O. S. Chauhan (2011), Climate induced variability of suspended matter and nutrient in the discharge of kali river, central west coast of India, *International Journal of Earth sciences and Engineering* (in press).
- Rixen, T., V. Ramaswamy, B. Gaye, B. Herunadi, E. Maier-Reimer, H. W. Bange, and V. Ittekkot (2009), Monsoonal and ENSO impact on particle fluxes and the biological pump in the Indian Ocean, in *Indian Ocean biogeochemical processes and ecological variability*, edited by J. D. Wiggert et al., Geophysical Monograph Series, American Geophysical Union, Washington, DC, USA, 185, pp. 365-383.
- SAC Report (2004) Atmospheric corrections, bio-optical algorithm development and validation of IRS-P4 OCM data (IRS-P4 OCM Utilisation/SATCORE Project Report). Scientific Report No. SATCORE/SAC/RESA/MWRG/SC/ 01/02, Space Application Center, Ahmedabad, pp. 98.

- Sardessai, S., N. Ramaiah, S. P. Kumar, and S. N. DeSousa (2007), Influence of environmental forcing on the seasonality of dissolved oxygen and nutrients in the Bay of Bengal, *J. Mar. Res.* 65(2), 301-316.
- Sarker, R. P. (1966), A dynamical model of orographic rainfall, *Mon. Wea. Rev.* 94, 555-572. doi: 10.1175/1520-0493(1966)094<0555:ADMOOR>2.3.CO;2.
- Shirodkar, P. V., A. Mesquita, U. K. Pradhan, X. N. Verlekar, M. T. Babu, and P. Vethamony (2009), Factors controlling physico-chemical characteristics in the coastal waters off Mangalore-A multivariate approach, *Environmental Research*, 109, 245-257, doi:10.1016/j.envres.2008.11.011.
- Strickland, S. C., and T. R. Parsons (1979), A Practical Handbook of Seawater Analyses. Bulletin of Fisheries Research Board of Canada, Ottawa.
- Tassan, S. (1994), Local algorithm using SeaWiFS data for retrieval of phytoplankton pigment, suspended sediments and yellow substances in coastal waters. *Appl. Opt.*, 12, 2369–2378. doi:10.1364/AO.33.002369.
- United Nations Educational, Scientific, and Cultural Organization (UNESCO) (1994), Protocols for the Joint Global Ocean Flux Study (JGOFS) Core Measurements, in *Manual and Guides*, Scientific committee on oceanic research, Paris, 29, pp. 170.
- Varkey M. J., V. Kesava Das G. N. Swamy, P. S. Joseph, and J. S. Sastry (1982), Wave (swell) atlas for Arabian sea and Bay of Bengal. Technical Report, National Institute of Oceanography, Dona-Paula, Goa, India. 385pp.
- Vörösmarty, C. J., B. Fekete, and B. A. Tucker (1996), River Discharge Database, Version 1.0 (RivDIS v1.0), Volumes 0 through 6. A contribution to IHP-V Theme 1, Technical Documents in Hydrology Series, UNESCO, Paris.
- Xie, S. P., Haiming Xu, N. H. Saji, Y. Wang, and W. T. Liu (2006), Role of Narrow Mountains in Large-Scale Organization of Asian Monsoon Convection, *J. Climate*, 19, 3420-3429. doi: 10.1175/JCLI3777.1.
- Xie, P., and P. A. Arkin (1997), Global precipitation: A 17-yr monthly analysis based on gauge observations, satellite estimates, and numerical model outputs, *B Am Meteorol Soc.*, 78, 2539–2558, doi: 10.1175/1520-0477(1997)078<2539:GPAYMA>2.0.CO;2.
- Yu, Z., and J. P. McCreary (2004), Assessing precipitation products in the Indian Ocean using an ocean model, *J Geophys Res.*, 109, C05,013. doi:10.1029/2003JC002,106, 2004.

## Figure Captions:

Figure 1. Location of the sampling stations and transects for the subsurface measurements. Averaged regional sea surface salinity (p.s.u.) during the SWM (2004) together with the topographic features of the Western Ghats (data source: <http://web.ics.purdue.edu/~braile/edumod/sv/1down.htm>) are shown in the inset. Shallow and deep (A-B) stations used for presentation of monthly variability of TSM (derived from imagery data) is also shown.

Figure 2. TSM distribution for the SWM (August 2004);(a) measured and (b) satellite derived. The panel (c) and (d) show measured and imagery derived TSM distribution respectively for the non-SWM seasons (January –February of 2011).

Figure 3. Month-scale imagery derived TSM (a&b) and chlorophyll-a (c&d) during 2003 and 2004. Refer to Figure 1 for the locations of transects. The enhanced turbidity, and higher productivity of the coastal waters is a conspicuous feature during the SWM.

Figure 4. Chlorophyll-a distribution: the SWM (August 2004;(a) measured and (b) imagery derived) and the non-SWM seasons (January –February of 2011; (c) measured and (d) imagery derived).

Figure 5. Nutrient ( $\text{NO}_3^-$ ,  $\text{PO}_4^{3-}$ ) distributions in the study area during the SWM (a & c) and during the non-SWM (b & d) seasons.

Figure 6. Spatial variability in dissolved oxygen levels during the SWM and the non-SWM seasons.

Figure 7. Vertical profiles of nitrate and dissolved  $\text{O}_2$  along three transects from the study area during the SWM. Refer to Fig. 1 for the locations of the each transect. Note a nutrient depletion in the subsurfaces in the inner shelf region, which is in contrast to the characteristic enrichment in nitrate and hypoxia in the deeper offshore waters.

Figure 8. Vertical distribution of nitrate and dissolved  $\text{O}_2$  along three transects from the study area during the non-SWM (January – February of 2011). Refer to Fig. 1 for the locations of the each transect.

Figure 9. Surface currents (A) and advective TSM vectors (B) in the study area during the SWM and the non-monsoon seasons.

Figure 10. Surface and vertical T-S profiles during the SWM (a-d) and the non-SWM seasons (e-h). *Note* a reduced salinity of surface and subsurface waters and elevated SST in the coastal waters during the SWM due to fluvial flux.

Figure 11. Averaged bimonthly wind regime in the study area during the SWM (a-b) and the non-SWM seasons (c-d) of 2004 (Data source: <ftp://ftp.ifremer.fr/pub/ifremer/cersat/products/gridded/mwf-quikscat/data/monthly/>).

Figure 12. Average surface sea level anomaly during the SWM (2004). (Data Source: <http://atoll-motu.aviso.oceanobs.com/?action=listcatalog&service=AvisoDT>).



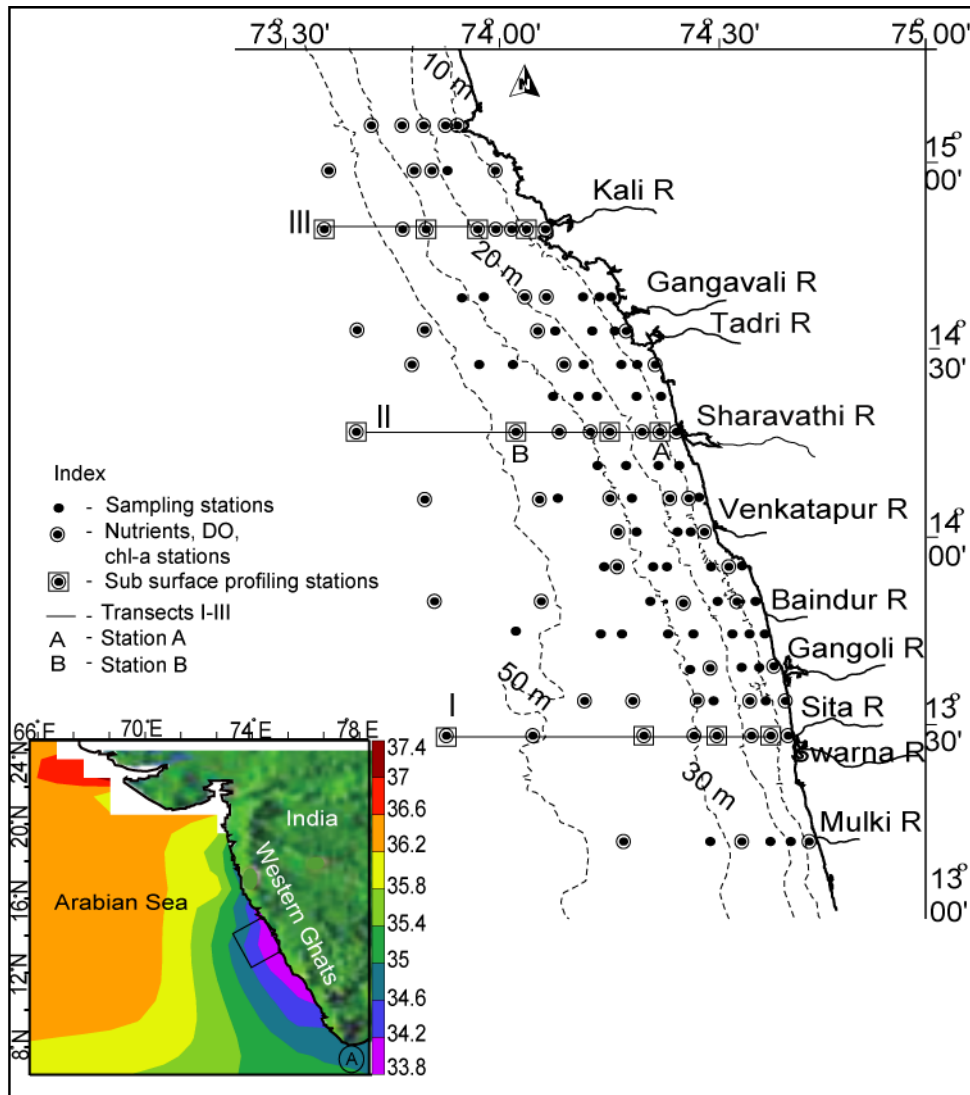


Figure 1. Location of the sampling stations and transects for the subsurface measurements. Averaged regional sea surface salinity (p.s.u.) during the SWM (2004) together with the topographic features of the Western Ghats (data source: <http://web.ics.purdue.edu/~braile/edumod/sv/1down.htm>) are shown in the inset. Shallow and deep (A-B) stations used for presentation of monthly variability of TSM (derived from imagery data) is also shown.

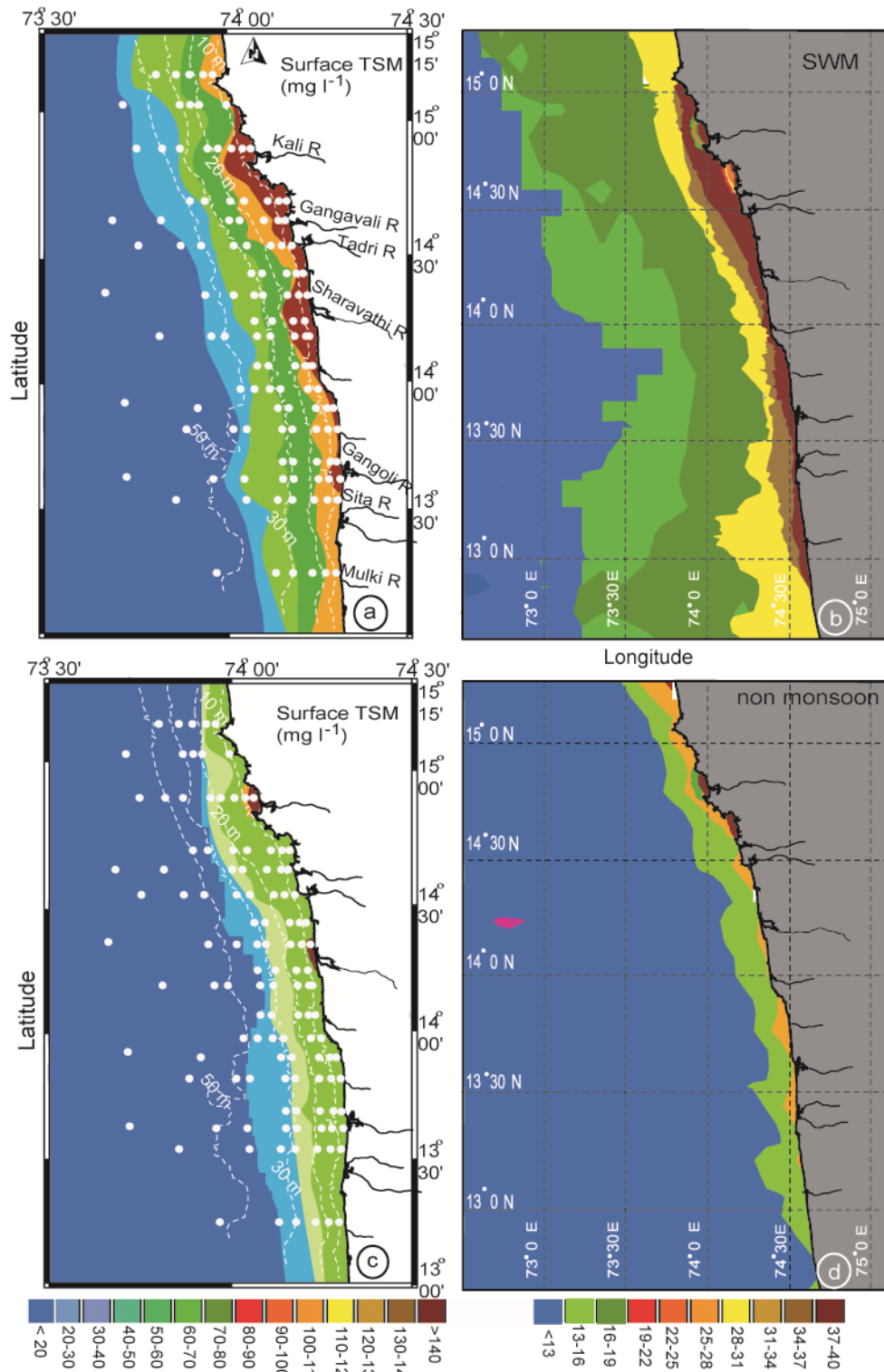


Figure 2. TSM distribution for the SWM (August 2004;(a) measured and (b) satellite derived. The panel (c) and (d) show measured and imagery derived TSM distribution respectively for the non-SWM seasons (January –February of 2011).

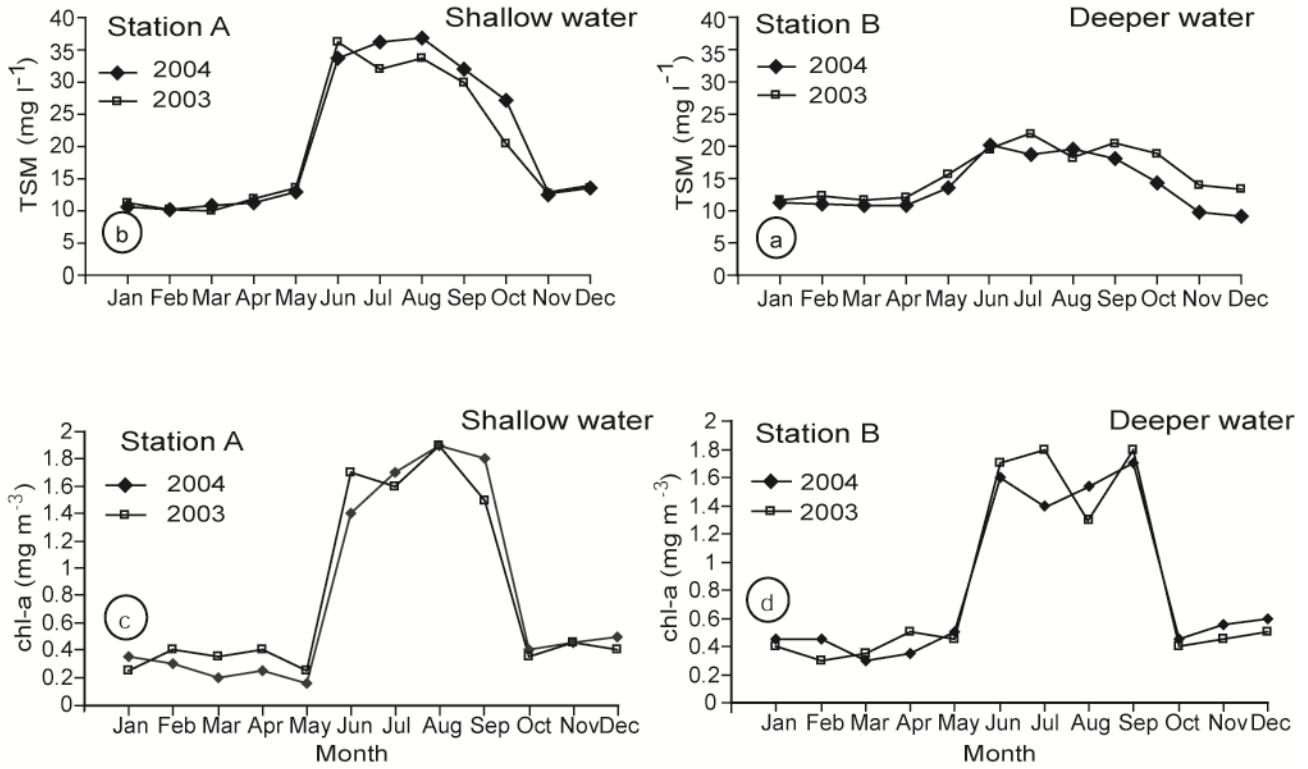


Figure 3. Month-scale imagery derived TSM (a&b) and chlorophyll-a (c&d) during 2003 and 2004. Refer to Figure 1 for the locations of transects. The enhanced turbidity, and higher productivity of the coastal waters is a conspicuous feature during the SWM.

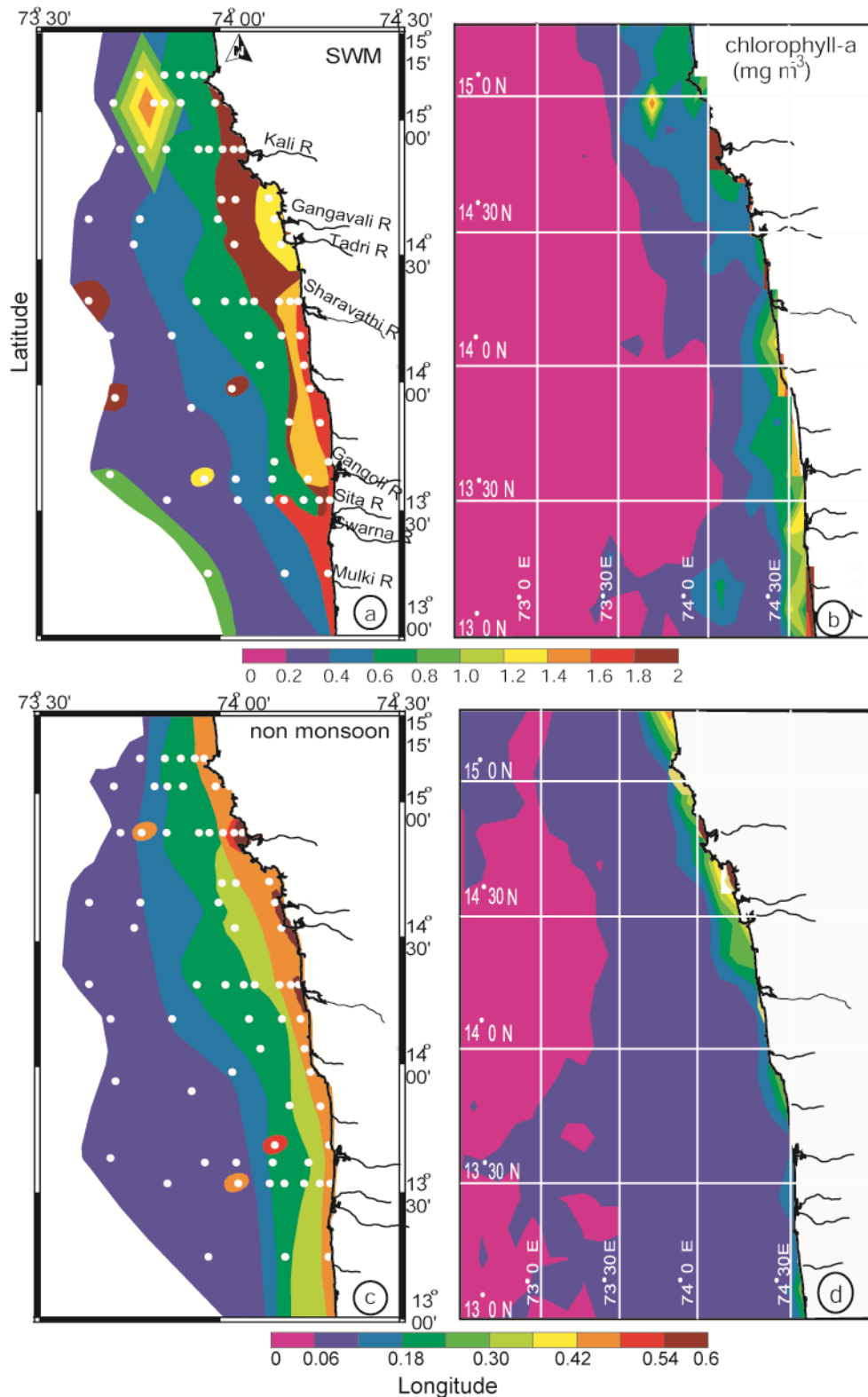


Figure 4. Chlorophyll-a distribution: the SWM (August 2004;(a) measured and (b) imagery derived) and the non-SWM seasons (January –February of 2011; (c) measured and (d) imagery derived).

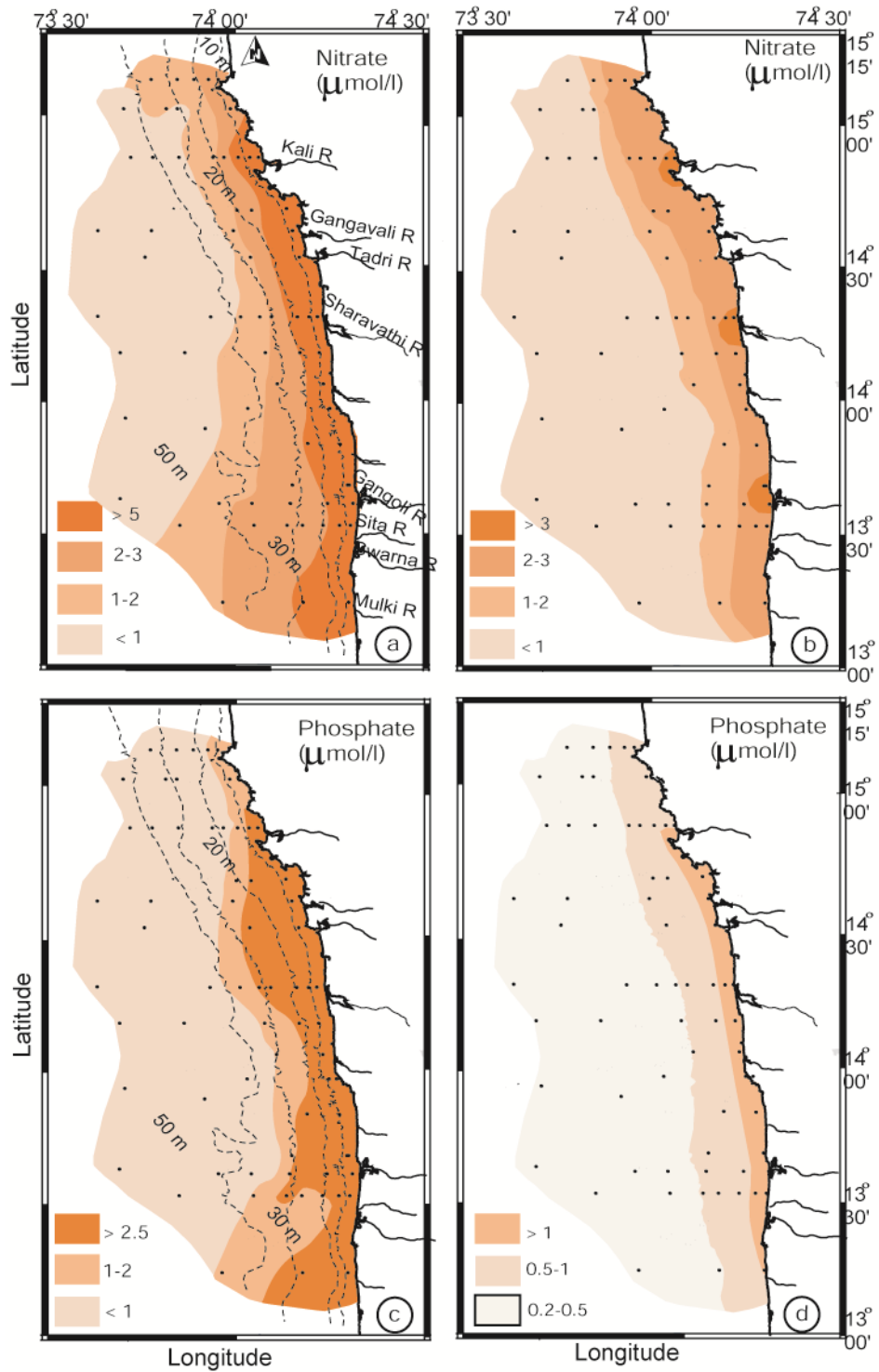


Figure 5. Nutrient ( $\text{NO}_3^-$ ,  $\text{PO}_4^{3-}$ ) distributions in the study area during the SWM (a & c) and during the non-SWM (b & d) seasons.

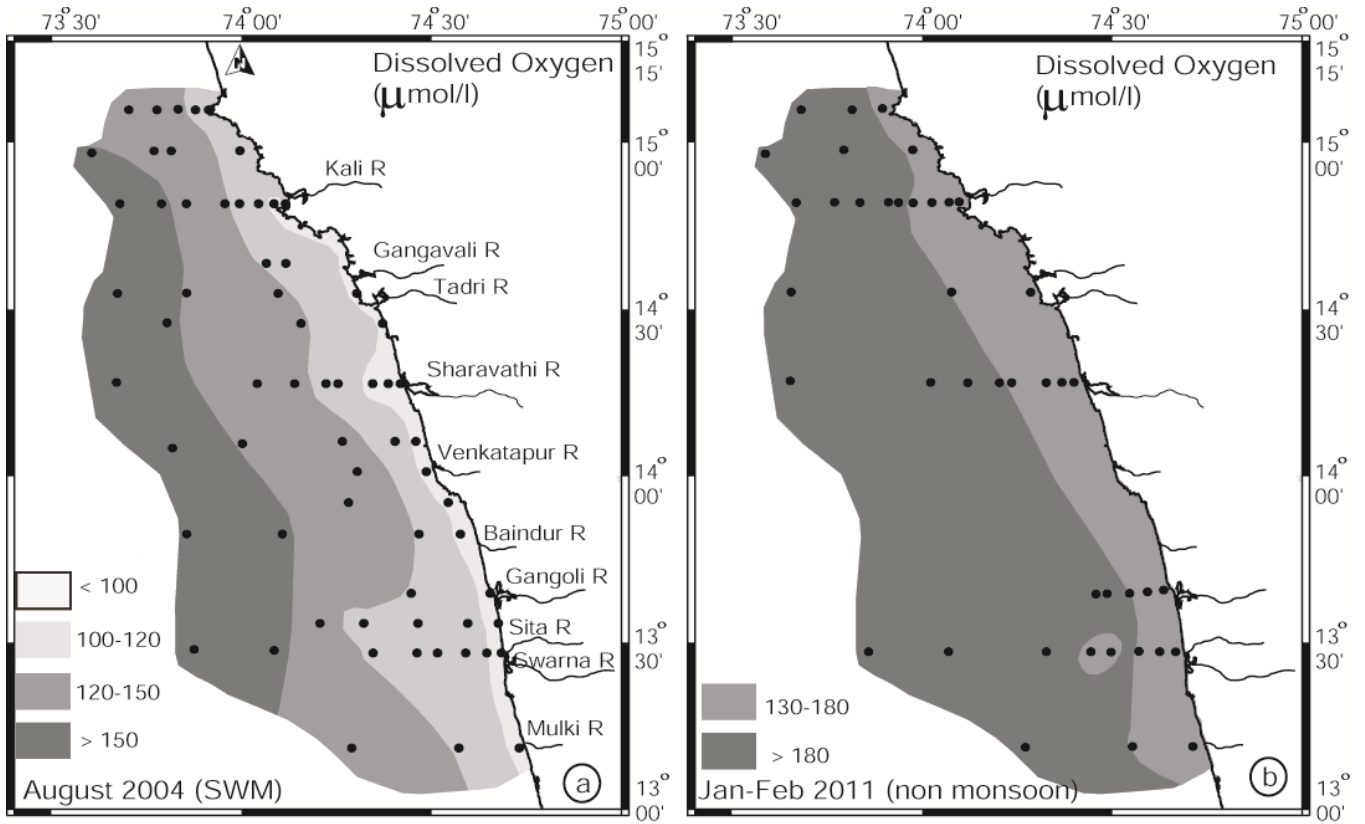


Figure 6. Spatial variability in dissolved oxygen levels during the SWM and the non-SWM seasons.

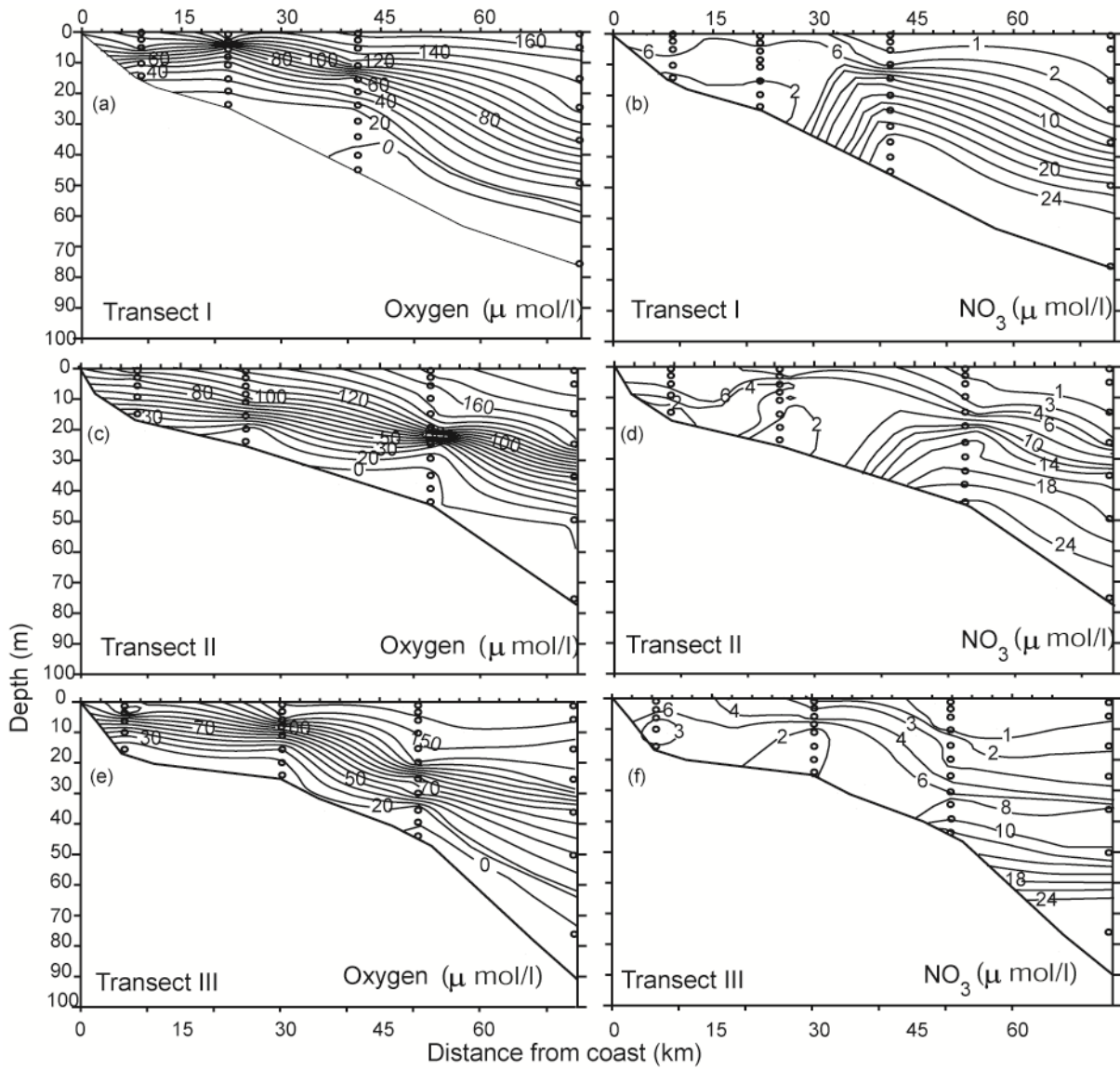


Figure 7. Vertical profiles of nitrate and dissolved O<sub>2</sub> along three transects from the study area during the SWM. Refer to Fig. 1 for the locations of the each transect. Note a nutrient depletion in the subsurfaces in the inner shelf region, which is in contrast to the characteristic enrichment in nitrate and hypoxia in the deeper offshore waters.

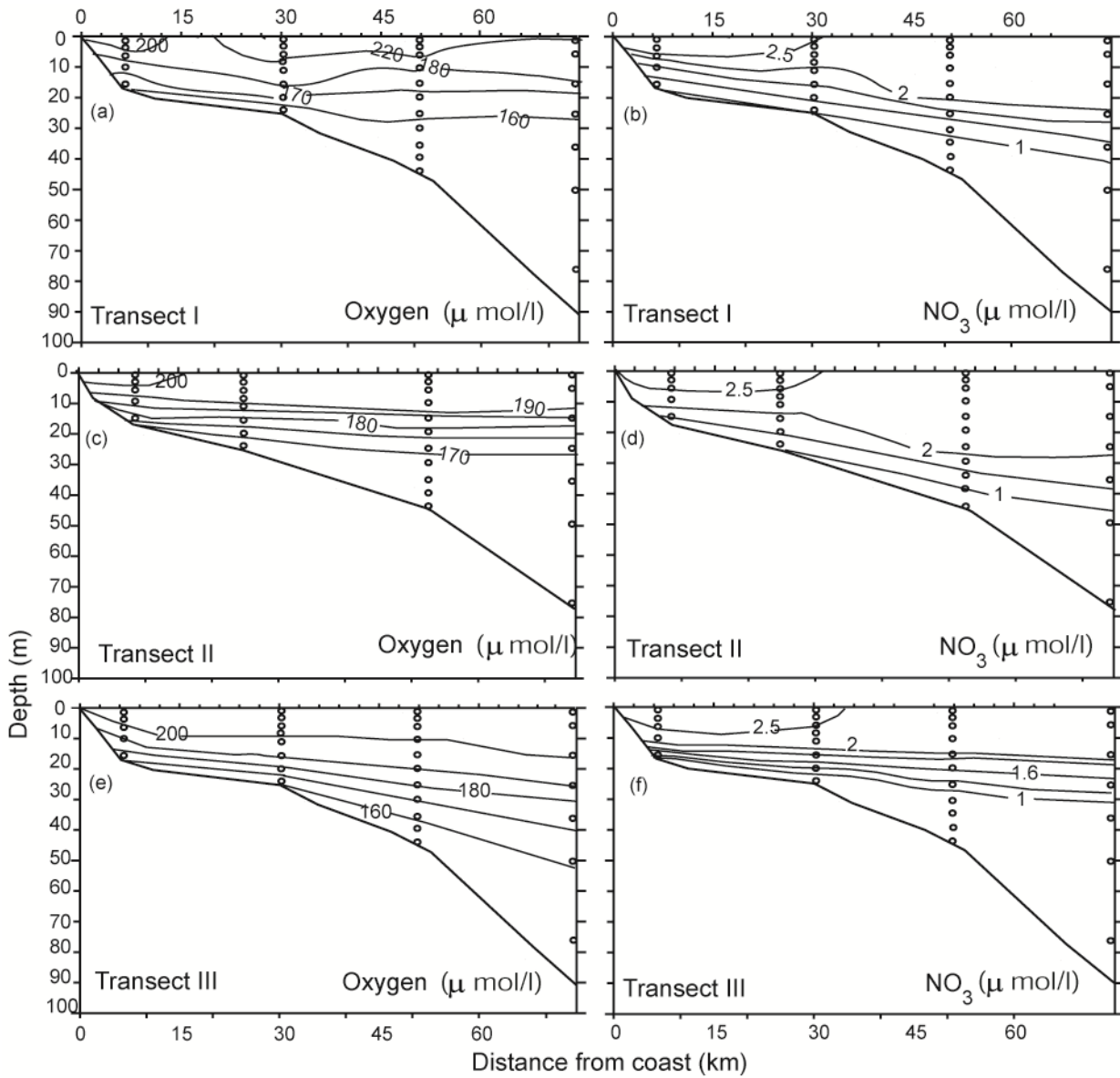


Figure 8. Vertical distribution of nitrate and dissolved O<sub>2</sub> along three transects from the study area during the non-SWM (January – February of 2011). Refer to Fig. 1 for the locations of the each transect.



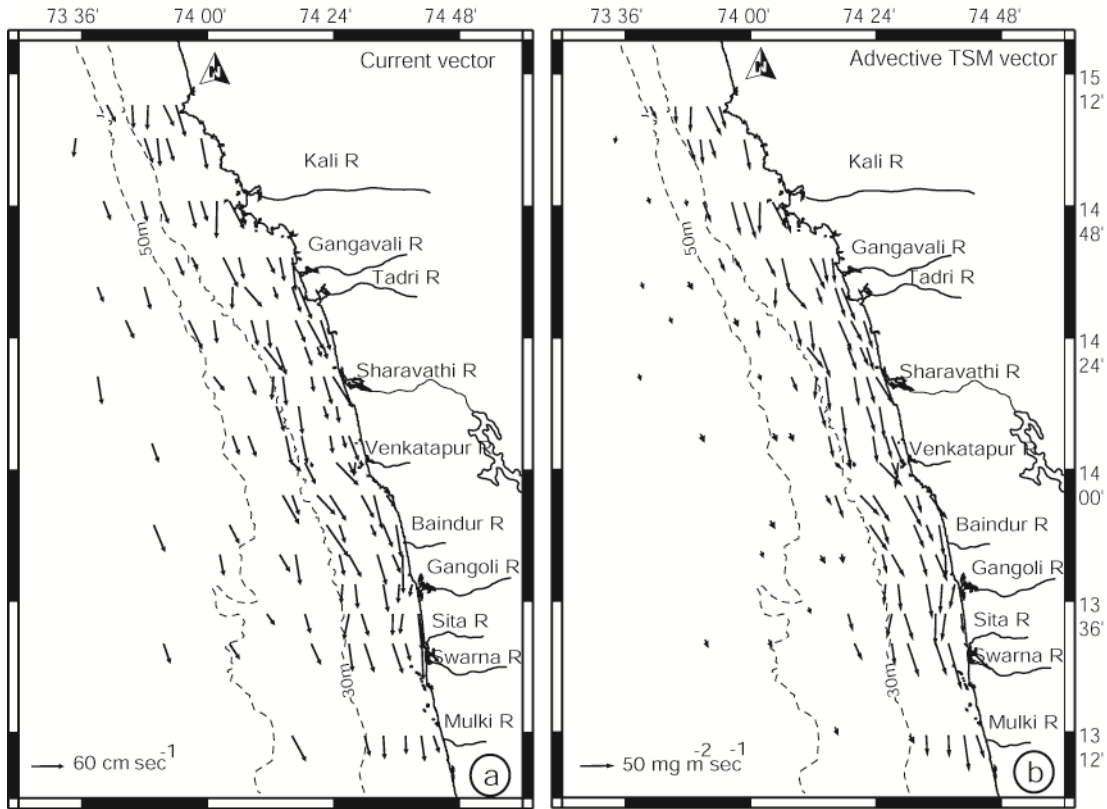


Figure 9. Surface currents (A) and advective TSM vectors (B) in the study area during the SWM and the non-monsoon seasons.

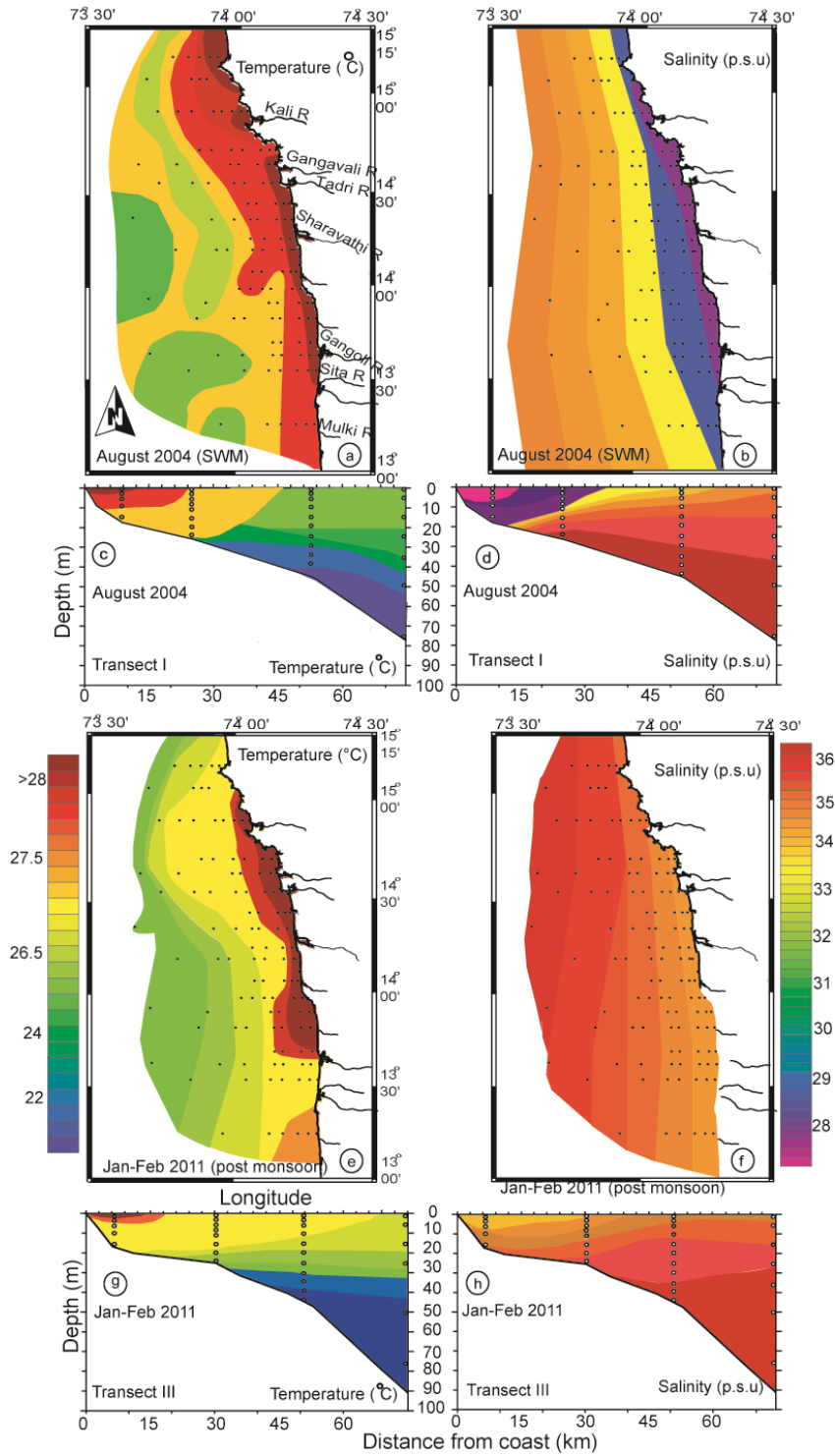


Figure 10. Surface and vertical T-S profiles during the SWM (a-d) and the non-SWM seasons (e-h). *Note* a reduced salinity of surface and subsurface waters and elevated SST in the coastal waters during the SWM due to fluvial flux.

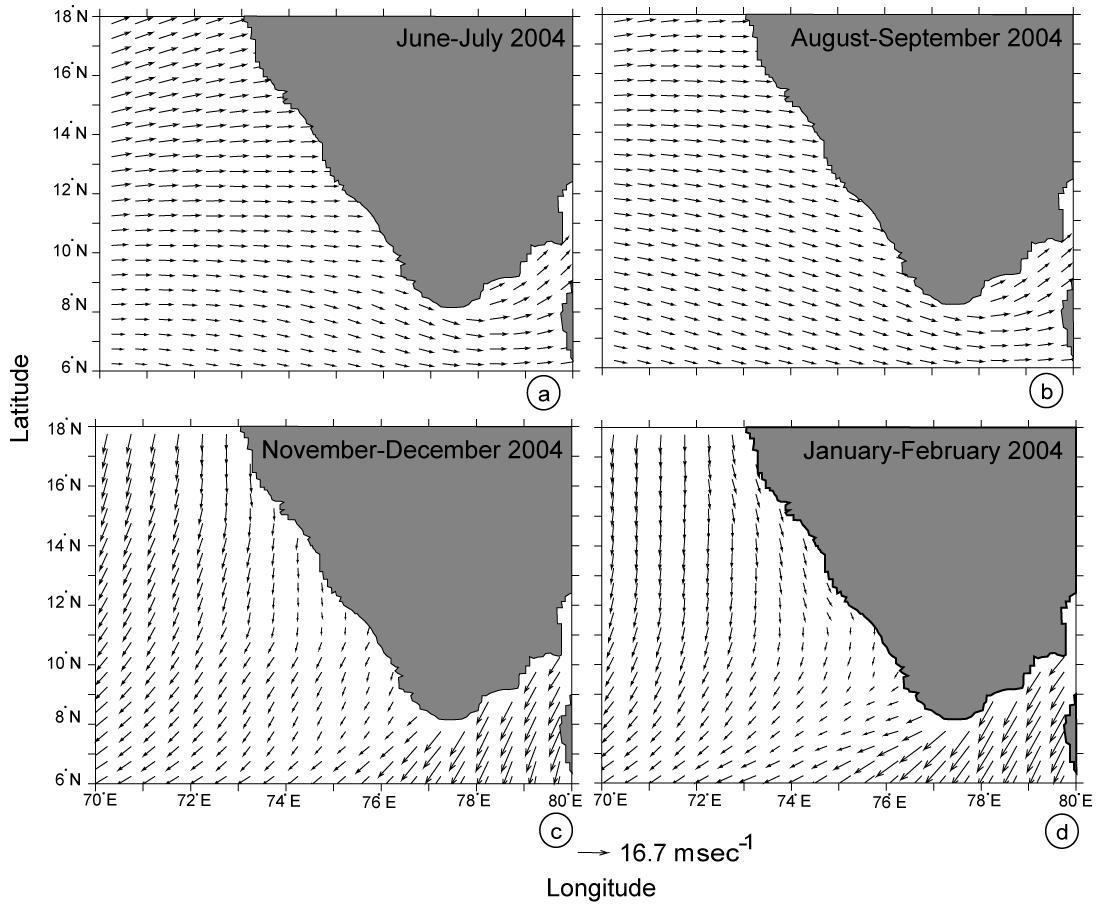


Figure 11. Averaged bimonthly wind regime in the study area during the SWM (a-b) and the non-SWM seasons (c-d) of 2004 (Data source: <ftp://ftp.ifremer.fr/pub/ifremer/cersat/products/gridded/mwf-quikscat/data/monthly/>).

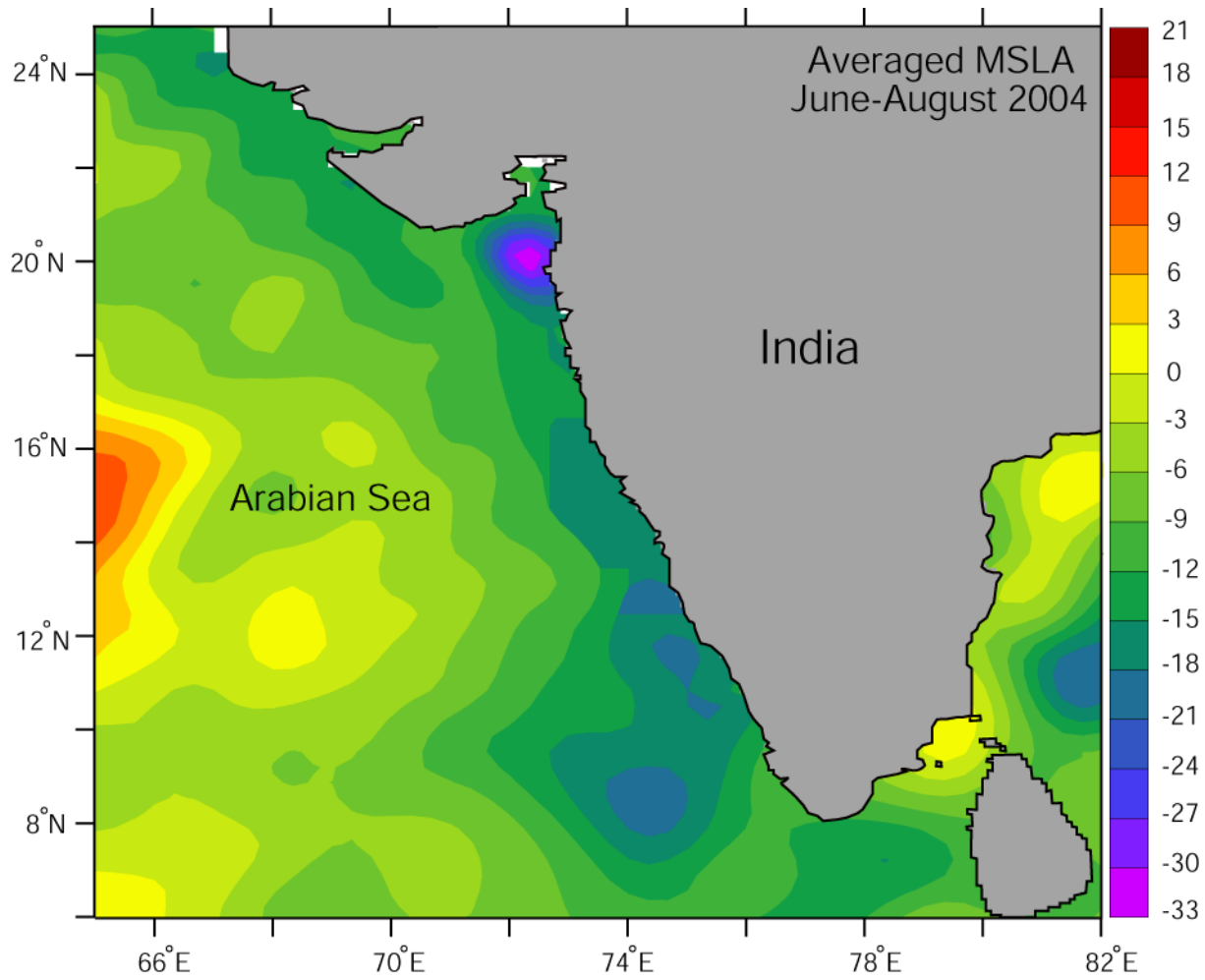


Figure 12. Average surface sea level anomaly during the SWM (2004). (Data Source: <http://atoll-motu.aviso.oceanobs.com/?action=listcatalog&service=AvisoDT>).